DMD Fast Forward. Published on April 16, 2021 as DOI: 10.1124/dmd.121.000439
This article has not been copyedited and formatted. The final version may differ from this version.

Investigating the Utility of Humanized PXR-CAR-CYP3A4/7 Mouse Model to Assess CYP3A-Mediated Induction

Justin Q. Ly, Susan Wong, Liling Liu, Ruina Li, Kirsten Messick, Jae H. Chang

JQL, SW, LL and KM: Genentech, INC, 1 DNA Way, South San Francisco, CA, 94080

JHC: ORIC Pharmaceuticals, 240 E Grand Ave, 2nd Floor, South Francisco, CA, 94080

DMD Fast Forward. Published on April 16, 2021 as DOI: 10.1124/dmd.121.000439
This article has not been copyedited and formatted. The final version may differ from this version.

Running Title: Humanized PXR-CAR-CYP3A4/7 Mouse as Model of Induction

Correspondence should be addressed to:

Jae H. Chang

Preclinical Development Sciences

ORIC Pharmaceuticals

240 E Grand Ave

South San Francisco, CA, 94080

Ph: (650) 388-5639

Email: jaechang@gmail.com

Number of text pages: 22

Number of tables: 3

Number of figures: 9 in 3 parts

Number of references: 42

Number of words in Abstract: 250

Number of words in Introduction: 885

Number of words in Discussion: 1526

DMD Fast Forward. Published on April 16, 2021 as DOI: 10.1124/dmd.121.000439
This article has not been copyedited and formatted. The final version may differ from this version.

Non-standard abbreviations:

ADR, adverse drug reaction; AUC, area under the curve; CAR, constitutive androstane receptor; Cavg, average concentration, Cmax, maximum concentration; CYP, cytochrome P450, DDI, drug-drug interaction; DME, drug metabolizing enzymes; EHC, enterohepatic circulation; k, enzymatic activity; LC-MS/MS, liquid chromatography-mass spectrometry; PBPK, physiological-based pharmacokinetic; PXR, pregnane X receptor; Tg-Composite, humanized PXR, CAR and CYP3A4/7

DMD Fast Forward. Published on April 16, 2021 as DOI: 10.1124/dmd.121.000439
This article has not been copyedited and formatted. The final version may differ from this version.

ABSTRACT

Clinical induction liability is assessed with human hepatocytes. However, underpredictions in the magnitude of clinical induction have been reported. Unfortunately, in vivo studies in animals do not provide additional insight due to species differences in drug metabolizing enzymes and their regulatory pathways. To circumvent this limitation, transgenic animals expressing human orthologues were developed. The aim of this work was to investigate the utility of mouse model expressing human orthologues of PXR, CAR and CYP3A4/7 (Tg-Composite) in evaluating clinical induction. Rifampin, efavirenz and pioglitazone, which were employed to represent strong, moderate and weak inducers, were administered at multiple doses to Tg-Composite animals. In vivo CYP3A activity was monitored by measuring changes in the exposure of the CYP3A probe substrate triazolam. Following the in vivo studies, microsomes were prepared from their livers to measure changes of in vitro CYP3A4 activity. In both in vivo and in vitro, distinction of clinic induction was recapitulated as rifampin yielded the greatest inductive effect following by efavirenz and pioglitazone. Interestingly, with rifampin, in vivo CYP3A activity was approximately 4-fold higher than in vitro activity. Conversely, there was no difference between in vivo and in vitro CYP3A activity with efavirenz. These findings are consistent with the report that while rifampin exhibits differential inductive effect between the intestines and liver, efavirenz does not. These data highlight the promise of transgenic models such as Tg-Composite to complement human hepatocytes to enhance the translatability of clinical induction as well as a powerful tool to further study mechanism of drug disposition.

DMD Fast Forward. Published on April 16, 2021 as DOI: 10.1124/dmd.121.000439
This article has not been copyedited and formatted. The final version may differ from this version.

Significance

Underprediction of the magnitude of clinical induction when using human hepatocytes have been reported, and transgenic models may improve clinical translatability. The work presented here showcases the Tg-Composite model which was able to recapitulate the magnitude of clinical induction and to differentiate tissue dependent induction observed with rifampin, but not with efavirenz. These results not only foreshadow the potential application of such transgenic models in assessing clinical induction, but also in further investigating the mechanism of drug disposition.

DMD Fast Forward. Published on April 16, 2021 as DOI: 10.1124/dmd.121.000439
This article has not been copyedited and formatted. The final version may differ from this version.

INTRODUCTION

The practice of polypharmacy has been on the rise, in part, due to advancements and breakthroughs that have been made in seeking remedies for assorted maladies. From 1999 to 2008, patients using more than one prescription drugs in the United States increased by 4.4-5.8% (CDC, October, 2010), and similar trend has been noted worldwide (Guthrie et al., 2015; Oktora et al., 2019). Despite the therapeutic advantage, one major drawback to patients taking multiple drugs is that the likelihood of eliciting adverse drug reaction (ADR) increases due to drug-drug interaction (DDI). It is estimated that ADR is responsible for approximately 6% of hospitalization (Lazarou et al., 1998; Pirmohamed et al., 2004), and that DDI constitutes 20% of reported events (Magro et al., 2012). Drugs can be eliminated by a variety of mechanisms, and among them, drug metabolism is responsible for eliminating >70% of drugs (Wienkers and Heath, 2005), of which the principal drug metabolizing enzyme (DME) is CYP3A (Shimada et al., 1994). For "victim" drugs that are substrates for CYP3A, unwanted outcomes of DDI can manifest in different ways such as when a "perpetrating" drug inhibits CYP3A to enhance the exposure of the victim drug to non-tolerated levels. In contrast, the perpetrating drug can induce DME activity to reduce the level of the victim drug to sub-therapeutic concentrations which renders the drug treatment ineffective. Consequently, one of the important considerations during drug research is to mitigate DDI liability of drug candidates.

The gold standard to assess potential clinical liability associated with CYP induction is human hepatocytes. However, there are uncertainties in translating in vitro hepatocyte data to the clinic as highlighted by high frequency of false positive and false negatives in retrospective analyses of clinically known inducers (Fahmi et al., 2010; Kenny et al., 2018). One reason for the poor outcome may be that the in vitro system is a static system that is unable to capture the dynamic

DMD Fast Forward. Published on April 16, 2021 as DOI: 10.1124/dmd.121.000439
This article has not been copyedited and formatted. The final version may differ from this version.

interaction that occurs at the molecular and physiological level. In addition, a perpetrating drug may exert differential effect in vitro which may both inhibit and induce DMEs, complicating translation to the clinic. While some success and much progress have been demonstrated with physiological-based pharmacokinetic (PBPK) modeling (Guo et al., 2013; Wagner et al., 2016), there continues to be challenges arising from uncertainty such as with measuring in vitro endpoints, finding relevant and appropriate scaling in vitro parameters, as well as incomplete characterization of in vivo disposition of compounds that are in early stages of clinical trials (Jones et al., 2015; Shebley et al., 2018; Peters and Dolgos, 2019). Consequently, it has been reported that PBPK can underpredict the magnitude of induction (Almond et al., 2016). While in vivo preclinical models may be able to bridge the gap between in vitro to the clinic, they are not typically employed because there can be striking species differences in the expression and activity of DMEs (Shimada et al., 1997; Nelson et al., 2004; Chu et al., 2013), as well as their regulatory pathways (Xie et al., 2000; Lu and Li, 2001).

To address the limitations around species differences in the expression and activity of proteins responsible for drug metabolism, genetically modified mouse models lacking endogenous murine DME and/or their regulatory genes, but expressing human orthologs of the corresponding genes, were developed. There have been several investigations with one such model, the transgenic mouse model expressing human orthologs of PXR, CAR and CYP3A4/3A7 (Tg-Composite), which showed that it was able to recapitulate the magnitude of inhibition and induction of marketed drugs (Chang et al., 2016; Ly et al., 2017). In addition to constitutive expression of CYP3A4 mRNA in the intestines and the liver of Tg-Composite animals, differential effect was demonstrated where rifampin exhibited a greater induction than pregnenolone-16a-carbonitrile on the expression of CYP3A4 in both the intestines and the liver,

DMD Fast Forward. Published on April 16, 2021 as DOI: 10.1124/dmd.121.000439
This article has not been copyedited and formatted. The final version may differ from this version.

and as triazolam levels decreased by 91% and 37% in the presence of rifampin and sulfinpyrazone, respectively; whereas no change was observed for pioglitazone (Hasegawa et al., 2011). While these studies have reported that transgenic models are able to recapitulate the extent of induction observed in the clinic, additional investigations are needed to further elucidate the relationship between in vitro parameters to in vivo, especially around how the in vitro parameters of induction are manifested in vivo. One powerful aspect of utilizing preclinical models is that from the same animal, both in vitro and in vivo parameters can be measured. The objective of this work was to further investigate the translatability of the Tg-Composite model to clinically observed DDI, particularly around induction. Studies were conducted to determine both in vitro and in vivo activity of CYP3A using triazolam as a probe substrate as it has been reported that in mouse, triazolam shows enhanced specificity towards human CYP3A compared with midazolam. Varying doses of rifampin, efavirenz and pioglitazone, which are categorized as strong, moderate and weak inducers, respectively (Shou et al., 2008; Zhang et al., 2014), were studied in Tg-Composite mouse using triazolam as the CYP3A probe substrate. In addition to assessing the effect of these inducers on triazolam exposure in vivo, livers were harvested from the animals to prepare microsomes where the in vitro CYP3A activity was measured. These data were used to evaluate the relationship between alterations of in vitro CYP3A activity to the extent of induction observed in vivo.

DMD Fast Forward. Published on April 16, 2021 as DOI: 10.1124/dmd.121.000439
This article has not been copyedited and formatted. The final version may differ from this version.

MATERIALS AND METHOD

Materials and Methods

Materials. Rifampin, efavirenz, triazolam, loperamide and indomethacin were purchased from Sigma-Aldrich (Milwaukee, Wisconsin, USA) whereas pioglitazone was purchased from Toronto Research Chemicals (Toronto, Canada). 1X Complete protease inhibitor was purchased from Roche Applied Sciences (Indianapolis, IN). All other chemicals and reagents were of analytical grade and were purchased from Sigma-Aldrich (St. Louis, MO).

Pharmacokinetic Study Design. Female transgenic mouse expressing human orthologs of PXR, CAR, CYP3A4/7 (Tg-Composite; Taconic Farms/Artemis, Cologne, Germany), were housed at controlled temperature and humidity in an alternating 12-hr light/dark cycle with access to food and water *ad libitum*. All in vivo studies were performed in accordance with Institutional Animal Care and Use Committee guidelines and in harmony with the Guide for Laboratory Animal Care and Use. Rifampin (3, 10, 30, or 100 mg/kg), efavirenz (5, 15, 50, or 250 mg/kg), pioglitazone (1, 5, 50, or 200 mg/kg), or vehicle, was administered orally to Tg-Composite animals for 5 days (N=4/group). All doses of the perpetrators were well tolerated. On the fifth day, a single 2 mg/kg oral dose of triazolam was administered to all animals in the studies. All compounds in this study were formulated in 10% DMSO/35% PEG400/55% water. Following administration of triazolam, blood samples were collected serially via talk nick at 0.25, 0.5, 1, 3, 6, and 8 hr post-dose. Blood (15 µL) was collected at each timepoint and diluted 4-fold with water containing 1.7 mg/mL of EDTA. All blood samples were stored at approximately -80°C until analysis. In addition to the blood collection, at approximately 8 hr post-dose, livers, which were used to prepare microsomes, were collected and stored at -80^{o}C.

DMD Fast Forward. Published on April 16, 2021 as DOI: 10.1124/dmd.121.000439
This article has not been copyedited and formatted. The final version may differ from this version.

Microsome Preparations. Livers collected from each animal in the PK study were used to prepare microsomes. Approximately one gram of whole liver was homogenized on ice with a Dounce glass A homogenizer (Kontes, Seattle, WA) in 1 mL of homogenization buffer containing 0.1 M potassium phosphate buffer (pH 7.4) with 250 mM sucrose, 1 mM EDTA, 0.1 mM DTT, 2 μg/mL leupeptin, 150 mM potassium chloride, 1X Complete protease inhibitor and freshly added 1 mM PMSF. The homogenate was centrifuged at 9,000 g for 20 min at 4°C, and the resulting supernatant was then centrifuged at 105,000 g for 60 min at 4°C in an ultracentrifuge. The resulting pellet was resuspended in 0.1 M potassium phosphate buffer (pH 7.4) containing 250 mM sucrose and stored at −80°C. Total microsomal protein concentration was determined using bicinchoninic acid (BCA) assay kit from Pierce (Rockford, IL).

Microsomal Incubation. A mixture containing previously prepared liver microsomes (0.1 mg/mL final protein concentration) in 0.1 M potassium phosphate buffer (PH 7.4) and NADPH (1 mM final concentration) were pre-incubated for 5 minutes at 37^0 C. Reactions were initiated with the addition of 1 μM triazolam in a total volume of 250 μL. Aliquots of 50 μL samples were collected at 0, 5, 15 and 30 minutes, and quenched in 100 μL acetonitrile containing loperamide as internal standard. Samples were centrifuge at 2,000 g for 10 minutes. Supernatant (80 μL) was transferred to an analytical plate and diluted 2-fold with water for LC-MS/MS analysis. All experiments were performed in triplicates.

Sample Analysis. The concentration of rifampin, efavirenz, pioglitazone and triazolam in mouse blood; and levels of triazolam from liver microsomal incubations, were quantified using a liquid chromatography-mass spectrometry/mass spectrometry (LC-MS/MS). The LC-MS/MS system was a Shimadzu Nexera (Columbia, MD, USA) system coupled to a QTRAP® 6500 mass spectrometer (AB Sciex, Foster City, CA, USA) equipped with a turbo-electrospray interface.

DMD Fast Forward. Published on April 16, 2021 as DOI: 10.1124/dmd.121.000439
This article has not been copyedited and formatted. The final version may differ from this version.

The aqueous mobile phase for all four analytes was water with 0.1% formic acid (A) and the organic mobile phase was acetonitrile with 0.1% formic acid (B). Chromatographic separations for rifampin, pioglitazone, and triazolam, were achieved with Kinetex 100A column (50x2.1mm, 1.6um F5). The gradient for these analytes increased from 10% B to 30% B in 3.5 minutes, and to 95% B in 1.3 minutes. This gradient was sustained for 0.7 minutes and was then decreased to 10% B within 0.01 minutes which was maintained for another 0.3 minutes. The flow rate was set at 0.8 mL/min and the cycle time (injection to injection including instrument delays) was approximately 5.8 minutes. Chromatographic separation of efavirenz was achieved with Kinetex XB-C18 100A column (30 × 2.1 mm, 2.6 μm). The gradient of efavirenz increased from 10% B to 90% B in 0.6 minutes which was sustained for 0.2 minutes. The gradient was then decreased to 10% B within 0.01 minutes which was maintained for another 0.2 minutes. The flow rate was 1.2 mL/min and the cycle time was approximately 1.0 minute. Quantitation was carried out using the multiple reactions monitoring (MRM) in the positive mode for rifampin (*m/z* 823.3 → 791.4), pioglitazone (357.0→ 134.1), triazolam (343.0 → 308.1), and loperamide (*m/z* 477.1 → 266.2) which was the internal standard for the positive ion mode. Negative mode was monitored for efavirenz (*m/z* 314.200 → 243.9) and indomethacin (*m/z* 356.0 → 312.0) which was the internal standard for the negative mode. Injection volume was 5 μL. The accuracy and precision for the back-calculated concentrations of the calibration curve was within ±25%. The lower limit of quantitation (LLOQ) for rifampin was 0.0182 μM, for efavirenz was 0.00230 μM, for pioglitazone was 0.0421 μM, and for triazolam was 0.00728 μM. All concentrations are reported as total concentrations.

Data Analysis. Area-under-the-blood concentration-time curve at the last timepoint (AUC_{tlast}) and maximum concentration (C_{max}) was determined by non-compartmental analysis using

DMD Fast Forward. Published on April 16, 2021 as DOI: 10.1124/dmd.121.000439
This article has not been copyedited and formatted. The final version may differ from this version.

Phoenix™ WinNonlin®, version 6.3 (Pharsight Corporation, Mountain View, CA). Average concentration (C_{avg}) was calculated by normalizing the AUC_{tlast} to the last sampling time of 8 hr, or to time when last concentration was determined. All data are reported as mean ($\pm$ SD) of four animals in each group.

Enzymatic rate of CYP3A4, k, was calculated by determining the half-life ($t_{1/2}$) of triazolam and using the following relationship:

$k = 0.693 / t_{1/2}$

Fold-increase of CYP3A4 activity in vivo was determined by calculating the ratio of triazolam AUC_{tlast} from animals that were treated with vehicle or perpetrators (i.e. AUC_{veh}/AUC_{treat}). Similarly, fold-increase of in vitro activity was determined by taking the ratio of CYP3A4 enzymatic rate that was determined from microsomes which was prepared from animals treated with perpetrator or vehicle (i.e. k_{treat}/k_{veh}). Ratios of AUC_{tlast} or k were plotted against in vivo exposures of perpetrators, and the effect-concentration relationship was described by a nonlinear regression curve fit with Prism 8.0 (GraphPad, San Diego, CA) using the following equation:

$E = E_{max} * X / (EC_{50}+X)$

where E is the inductive effect of the perpetrator calculated as ratio of AUC_{tlast} or k, E_{max} is the maximum induction, EC_{50} is the concentration of perpetrator which elicits half of E_{max} and X is the observed in vivo concentration of the perpetrators.

DMD Fast Forward. Published on April 16, 2021 as DOI: 10.1124/dmd.121.000439
This article has not been copyedited and formatted. The final version may differ from this version.

RESULTS

Pharmacokinetics of rifampin, efavirenz and pioglitazone in Tg-Composite animals

Following 5 days of daily oral administration, the exposure of perpetrating drugs was determined in Tg-Composite animals. Exposures of rifampin, efavirenz and pioglitazone, as determined by AUC_{tlast}, C_{max} and C_{avg}, are summarized in Table 1. Following oral administration of rifampin, exposures increased with increasing doses from 3 mg/kg to 100 mg/kg. At 100 mg/kg, exposures were greater than dose proportional. Blood concentration-time profile in Figure 1A shows that rifampin was slowly eliminated. Following oral administration of efavirenz, the blood concentration-time profile in Figure 1B shows that efavirenz was rapidly eliminated. Oral exposures increased with increasing doses from 5 mg/kg to 250 mg/kg. At the highest dose of 250 mg/kg, exposures were less than dose proportional, therefore, higher doses were not investigated. Following oral administration of pioglitazone, exposures increased with increasing doses from 1 mg/kg to 200 mg/kg. At the highest dose of 200 mg/kg, exposures were less than dose proportional. Blood concentration-time profiles in Figure 1C shows that pioglitazone was rapidly eliminated.

Inductive effect of rifampin, efavirenz and pioglitazone as measured by changes in the oral exposure of triazolam in Tg-Composite animals

Magnitude of induction was measured by assessing the change of AUC_{tlast} of CYP3A probe substrate triazolam following 5-day oral administration of rifampin, efavirenz and pioglitazone, at several dose strengths in Tg-Composite animals. Based on the half-life of CYP3A protein of approximately 1 day, it was assumed that 5-day administration of the perpetrators were adequate to achieve steady-state expression of CYP3A (Yang et al., 2008; Ramsden et al., 2015; Takahashi et al., 2017). While midazolam is typically used as a probe substrate for CYP3A in

DMD Fast Forward. Published on April 16, 2021 as DOI: 10.1124/dmd.121.000439
This article has not been copyedited and formatted. The final version may differ from this version.

the clinic, it has been shown that it is extensively metabolized by endogenous mouse Cyp2c (van Waterschoot et al., 2008), precluding its utility in studies involving transgenic mouse models. Instead, triazolam was chosen as a probe substrate because enhanced specificity towards human CYP3A was previously demonstrated (Perloff et al., 2000). Triazolam in human is rapidly eliminated by metabolism mediated by CYP3A with a half-life of approximately 3 hr (Kinirons et al., 1996). Similarly, the half-life of triazolam in the Tg-Composite model was approximately 2 hr.

Table 2 summarizes the impact of rifampin, efavirenz and pioglitazone, on in vivo CYP3A activity by assessing the change of triazolam AUC_{tlast} in the absence and presence of perpetrators (AUC_{veh}/AUC_{treat}). When compared to vehicle treated group, triazolam AUC_{tlast} decreased by 2.78-, 13.0-, 24.6- and 44.9-fold, in the presence of ascending doses of rifampin at 3, 10, 30 and 100 mg/kg, respectively, where the AUC was 0.643, 4.62, 14.1 and 141 µM*hr, respectively; and Cmax was 0.0963, 0.655, 2.33 and 25.1 µM, respectively. When triazolam AUC ratios were plotted against Cmax and Cavg values determined for rifampin in vivo (Figure 2A), triazolam AUC ratios plateaued despite rifampin exposures continuing to increase to yield EC50 and Emax values of 1.76 µM and 49.2, when using Cavg values, respectively; and 2.24 µM and 48.6, when using Cmax values, respectively (Table 3). Following administration of efavirenz, triazolam AUC_{tlast} decreased by 1.05-, 1.42-, 1.90- and 5.59-fold relative to the vehicle treated group, at efavirenz doses of 5, 15, 50 and 250 mg/kg, respectively, where the AUC was 0.0217, 0.112, 1.06 and 2.29 µM*hr, respectively; and Cmax was 0.0561, 0.150, 0.933 and 2.46 µM, respectively. However, because triazolam AUC ratios continued to increase with increasing exposure of efavirenz, EC50 and Emax values were not determined (Figure 2B). Unlike rifampin and efavirenz, pioglitazone only had a modest impact on triazolam AUC_{tlast} as

DMD Fast Forward. Published on April 16, 2021 as DOI: 10.1124/dmd.121.000439
This article has not been copyedited and formatted. The final version may differ from this version.

pioglitazone reduced triazolam AUC_{tlast} by 1.17-, 1.19-, 1.43- and 1.61-fold relative to the vehicle group, at pioglitazone doses of 1, 5, 50 and 250 mg/kg, respectively, where the AUC was 03.82, 11.0, 54.5 and 104 µM*hr, respectively; and Cmax was 1.19, 4.6, 16.7 and 32.0 µM, respectively. Figure 2C shows that triazolam AUC_{tlast} ratios reached saturation despite pioglitazone exposures continuing to increase to yield EC50 and Emax values of 7.09 µM and 1.89, when using Cavg values, respectively; and 27.5 µM and 2.08, when using Cmax values, respectively (Table 3).

In vitro activity in liver microsomes prepared from Tg-Composite animals treated with rifampin, efavirenz and pioglitazone

To further characterize the inductive potential of rifampin, efavirenz and pioglitazone, in vitro metabolism of triazolam was assessed in microsomes prepared from livers that were harvested from the animals employed in the in vivo study. Table 2 summarizes the modulation of in vitro CYP3A activity by assessing the fold-increase of triazolam enzymatic rate in the presence and absence of perpetrators (k_{treat}/k_{veh}). When compared with vehicle treated group, in vitro CYP3A activity was increased by 2.75-, 4.75-, 9.87- and 11.0-fold, from microsomes where Tg-Composite animals were administered 3, 10, 30 and 100 mg/kg, respectively. Fold-change of in vitro CYP3A activity was plotted against Cmax and Cavg values determined for rifampin in vivo. Figure 3A shows that the fold-change of in vitro CYP3A activity reached saturation with increasing exposure of rifampin to yield EC50 and Emax values of 0.708 µM and 11.8, when using Cavg values, respectively; and 0.882 µM and 11.8, when using Cmax values, respectively (Table 3). For efavirenz, relative to vehicle treated animals, in vitro CYP3A activity increased by 0.978-, 1.19-, 2.08- and 4.22-fold, from microsomes where Tg-Composite animals were administered 5, 15, 50 and 250 mg/kg, respectively. Because in vitro CYP3A activity continued

DMD Fast Forward. Published on April 16, 2021 as DOI: 10.1124/dmd.121.000439
This article has not been copyedited and formatted. The final version may differ from this version.

to increase with increasing doses of efavirenz (Figure 3B), EC50 and Emax values were not determined. For pioglitazone, relative to vehicle treated animals, in vitro CYP3A activity increased by 1.07-, 1.17-, 1.52- and 1.66-fold, from microsomes where Tg-Composite animals were administered pioglitazone doses of 1, 5, 50 and 200 mg/kg, respectively. Figure 3C shows that fold-change of in vitro CYP3A activity reached saturation to yield EC50 and Emax values of 5.99 µM and 1.97, when using Cavg values, respectively; and 20.5 µM and 2.10, when using Cmax values, respectively (Table 3).

DMD Fast Forward. Published on April 16, 2021 as DOI: 10.1124/dmd.121.000439
This article has not been copyedited and formatted. The final version may differ from this version.

DISCUSSION

The aim of the current work was to investigate the effect of rifampin, efavirenz and pioglitazone, on the induction of the CYP3A probe substrate triazolam in transgenic model expressing human orthologues of PXR, CAR and CYP3A4/7 (Tg-Composite). Several dose levels of the perpetrators were administered to explore the link between dose and the degree of induction. In addition to monitoring modulation of triazolam exposures in vivo, microsomes prepared from livers of the animals in the in vivo studies were used to determine the impact on in vitro activity. Rifampin represented the strong inducer used in this study. Exposure of rifampin increased with increasing doses of rifampin which enabled exploration of concentration-induction response, and reached clinically relevant exposure by 100 mg/kg (Burger et al., 2006). At the highest administered dose of 100 mg/kg, CYP3A activity was 4-fold higher in vivo than in vitro. Accordingly, when these data were fit to a concentration-response curve using in vivo exposures determined for rifampin, Emax was approximately 4-fold higher in vivo than in vitro, accompanied by 2.5-fold shift in EC50. EC50 and Emax determined from microsomes from the Tg-Composite animals were comparable to literature values from human hepatocytes (Shou et al., 2008; Zhang et al., 2014), and when using the parameters determined at 100 mg/kg rifampin to calculate R3 from the static model (FDA, 2020), R3 value was 0.09 (fraction unbound in mouse plasma determined internally was 0.022). However, this R3 value markedly underpredicted the induction observed in vivo where there was 44.9-fold decrease (or observed ratio of 0.02) in triazolam AUC. However, despite the disconnect of CYP induction between in vivo and in vitro, these results are consistent with the report that rifampin has a greater inductive effect on the intestine than the liver (Fromm et al., 1996), where rifampin exerted 5- to 11-fold higher induction of midazolam when it was administered orally than intravenously (Gorski et al.,

DMD Fast Forward. Published on April 16, 2021 as DOI: 10.1124/dmd.121.000439
This article has not been copyedited and formatted. The final version may differ from this version.

2003; Kharasch et al., 2004; Kirby et al., 2011). In fact, one reason why rifampin may exhibit differential inductive effect between the liver and the intestine is because rifampin undergoes extensive enterohepatic circulation (EHC) (RIFADIN, 2020). EHC could theoretically augment the mean residence time of rifampin in the intestine to exert a greater inductive effect in the intestine. Therefore, rather than nullifying the utility of the Tg-Composite model, the disconnect highlights the potential advantage of such humanized animal models, while revealing limitation of human hepatocytes to translate to the clinic for orally administered drugs. Particularly, underprediction of how DDI manifests is not ideal and can compromise the safety of patients. This work insinuates that by being able to capture the physiological disposition of the drug and intestinal contribution of induction, Tg-Composite model may be able to improve the translatability to the clinic by integrating parameters such as EHC and first-pass effect which cannot be done with human hepatocytes.

In contrast, the degree of induction observed for efavirenz, which represents the moderate inducer used in this study (Shou et al., 2008), was comparable between in vitro and in vivo across all examined doses, implying that efavirenz yields similar effects on the intestines and the liver. Indeed, these data are congruent with the finding that unlike rifampin, efavirenz does not exhibit differential inductive effect on the intestines and the liver (Mouly et al., 2002). Taken together with rifampin data, these results indicate that Tg-Composite model is able to differentiate between the various type of induction that may be exerted differently by perpetrators. Additional experiments, including in vivo experiments following intravenous administration of triazolam as well as examining activity in enterocytes will be valuable in further investigating the potential differences in tissue-dependent induction between rifampin and efavirenz. Current in vitro methodology and tools such as PBPK are unable to account for

DMD Fast Forward. Published on April 16, 2021 as DOI: 10.1124/dmd.121.000439
This article has not been copyedited and formatted. The final version may differ from this version.

tissue-dependent response a priori, but such understanding is vital in improving the translatability to the clinic. This work is not proposing to move completely away from evaluating induction liability with human hepatocytes. Instead, data show that transgenic animals may be able to complement the current workflow to enhance the predictability of in vitro parameters associated with induction, especially if in vitro data indicate that there is a likelihood of meaningful induction. One caveat to the data with efavirenz was that although exposures increased with increasing doses, the exposures were below clinical exposures (SUSTIVA, 2015). Consequently, because CYP activity continued to rise, Emax could not be defined. This points to one of the drawbacks of Tg-Composite model which is that while some proteins are humanized, the disposition of compounds are controlled mostly by endogenous murine machinery, and that the compound may not be well tolerated in the transgenic animals. Therefore, dosing strategy of the perpetrator must be carefully considered, and it may be that in vivo testing may be limited by insufficient in vivo exposure and/or imperfect tolerability of the compound.

Pioglitazone represented the weak inducer in this study, and it was gratifying to see that the Tg-Composite model was able to capture the weak induction. Exposures of pioglitazone increased with increasing doses and reached clinically relevant exposure by 50 mg/kg (Budde et al., 2003). EC50 and Emax determined from microsomes from the Tg-Composite animals were comparable to literature values from human hepatocytes (Zhang et al., 2014), and when using the parameters determined at 200 mg/kg pioglitazone, R3 value was 0.6 (fraction unbound in mouse plasma determined internally was 0.007). However, unlike rifampin, this R3 value was comparable to what was observed in vivo where there was 1.61-fold decrease (or observed ratio of 0.6) in triazolam AUC.

DMD Fast Forward. Published on April 16, 2021 as DOI: 10.1124/dmd.121.000439
This article has not been copyedited and formatted. The final version may differ from this version.

For in vitro assessment, the current regulatory guidance recommends monitoring mRNA rather than CYP activity based on the evidence that there is a higher frequency of false negatives when considering CYP activity (Fahmi et al., 2010). Unfortunately, due to the small size of the mouse liver, there was only samples to measure CYP3A activity in the current study. However, it has been reported that in the absence of time-dependent inhibition, in vitro CYP activity can be equally valuable (Kenny et al., 2018). Because rifampin and efavirenz are not time-dependent inhibitors and because pioglitazone is a relatively weak time-dependent inhibitor, the current analysis using in vitro CYP3A activity is suitable. However, there is merit in investigating mRNA in future experiments as it would continue to build foundation around the Tg-Composite models so that it can be used to evaluate new molecular entities whose induction liability is not well characterized.

In summary, Tg-Composite model successfully differentiated the differing degree of induction reported for rifampin, efavirenz and pioglitazone. The range of modulation of CYP3A activity was large enough to mirror the strong induction mediated by rifampin but also sensitive enough to recapitulate the weak induction of pioglitazone. There are several advantages of Tg-Composite model to assess clinical induction. First, in vivo models afford physiological elements that are absent from a static in vitro model which allows for the data to be bridged to the clinic more effectively. For example, it was shown that intestinal contribution to induction, which may be substantial for perpetrators such as rifampin, was appropriately integrated in the Tg-Composite animals. Another benefit is that Tg-Composite models enable further investigation into the physiological mechanism of induction. For example, the ability to evaluate both in vitro and in vivo parameters from the same animals enabled examination on how to best scale in vitro data. Specifically, this work showed that in vitro values mirrored in vivo

DMD Fast Forward. Published on April 16, 2021 as DOI: 10.1124/dmd.121.000439
This article has not been copyedited and formatted. The final version may differ from this version.

modulation of CYP3A activity, and that induction is driven by AUC. Furthermore, analysis of in vitro and in vivo data revealed that there was tissue-dependent induction mediated by rifampin but not by efavirenz. Findings with Tg-Composite model address some of the gaps of using hepatocytes and show promise in improving the translatability of preclinical data to assess the clinical induction liability of new chemical entities. Currently, it is challenging to gauge the worth of these models in informing drug research since not much data are yet available. However, effort was required to evaluate the value of genetically altered animal models in scientific areas such as biology and toxicology, and eventually, the merit of the genetically modified models was demonstrated. As a result, these models were adopted into their workflows and have revolutionized how these scientific disciplines conduct drug research. Similarly, models such as Tg-Composite are emerging models that may aid in the study of drug disposition, and there may be a benefit in exploring the utility of these models further. In conclusion, these results show that Tg-Composite model was able to recapitulate the extent of clinical induction and establish that increases in CYP3A activity was driven at the molecular level in liver microsomes. While additional work is needed to fully characterize induction mediated by PXR and CAR, this is one of the first work which describes the extent of in vitro and in vivo induction derived from the same animal which is valuable in establishing in vitro to in vivo correlation. The current work demonstrates that Tg-Composite model is a relevant tool that can complement existing assessments of clinical induction such as with human hepatocytes to enhance the translatability of clinical induction as well as a powerful tool to further study mechanism of drug disposition.

DMD Fast Forward. Published on April 16, 2021 as DOI: 10.1124/dmd.121.000439
This article has not been copyedited and formatted. The final version may differ from this version.

Authorship contribution

Participated in research design: Ly, Wong, Chang

Conducted experiments: Ly, Liu, Li, Messick, Wong

Performed data analysis: Ly, Liu, Li, Wong, Chang

Wrote or contributed to the writing of the manuscript: Ly, Wong, Chang

DMD Fast Forward. Published on April 16, 2021 as DOI: 10.1124/dmd.121.000439
This article has not been copyedited and formatted. The final version may differ from this version.

References

Almond LM, Mukadam S, Gardner I, Okialda K, Wong S, Hatley O, Tay S, Rowland-Yeo K, Jamei M, Rostami-Hodjegan A, and Kenny JR (2016) Prediction of Drug-Drug Interactions Arising from CYP3A induction Using a Physiologically Based Dynamic Model. *Drug Metab Dispos* **44:**821-832.

Budde K, Neumayer HH, Fritsche L, Sulowicz W, Stompor T, and Eckland D (2003) The pharmacokinetics of pioglitazone in patients with impaired renal function. *Br J Clin Pharmacol* **55:**368-374.

Burger DM, Agarwala S, Child M, Been-Tiktak A, Wang Y, and Bertz R (2006) Effect of rifampin on steady-state pharmacokinetics of atazanavir with ritonavir in healthy volunteers. *Antimicrob Agents Chemother* **50:**3336-3342.

CDC (October, 2010) Prescription Drug Use Continues to Increase: U.S. Prescription Drug Data for 2007–2008.

Chang JH, Chen J, Liu L, Messick K, and Ly J (2016) Rifampin-Mediated Induction of Tamoxifen Metabolism in a Humanized PXR-CAR-CYP3A4/3A7-CYP2D6 Mouse Model. *Drug Metab Dispos* **44:**1736-1741.

Chu X, Bleasby K, and Evers R (2013) Species differences in drug transporters and implications for translating preclinical findings to humans. *Expert Opin Drug Metab Toxicol* **9:**237-252.

Fahmi OA, Kish M, Boldt S, and Obach RS (2010) Cytochrome P450 3A4 mRNA is a more reliable marker than CYP3A4 activity for detecting pregnane X receptor-activated induction of drug-metabolizing enzymes. *Drug Metab Dispos* **38:**1605-1611.

FDA (2020) In Vitro Drug Interaction Studies--Cytochrome P450 Enzyme and Transporter-Mediated Drug Interactions: Guidance for Industry ((CDER) CfDEaR ed.

Fromm MF, Busse D, Kroemer HK, and Eichelbaum M (1996) Differential induction of prehepatic and hepatic metabolism of verapamil by rifampin. *Hepatology* **24:**796-801.

Gorski JC, Vannaprasaht S, Hamman MA, Ambrosius WT, Bruce MA, Haehner-Daniels B, and Hall SD (2003) The effect of age, sex, and rifampin administration on intestinal and hepatic cytochrome P450 3A activity. *Clin Pharmacol Ther* **74:**275-287.

Guo H, Liu C, Li J, Zhang M, Hu M, Xu P, Liu L, and Liu X (2013) A mechanistic physiologically based pharmacokinetic-enzyme turnover model involving both intestine and liver to predict CYP3A induction-mediated drug-drug interactions. *J Pharm Sci* **102:**2819-2836.

Guthrie B, Makubate B, Hernandez-Santiago V, and Dreischulte T (2015) The rising tide of polypharmacy and drug-drug interactions: population database analysis 1995-2010. *BMC Med* **13:**74.

Hasegawa M, Kapelyukh Y, Tahara H, Seibler J, Rode A, Krueger S, Lee DN, Wolf CR, and Scheer N (2011) Quantitative prediction of human pregnane X receptor and cytochrome P450 3A4 mediated drug-drug interaction in a novel multiple humanized mouse line. *Mol Pharmacol* **80:**518-528.

Jones HM, Chen Y, Gibson C, Heimbach T, Parrott N, Peters SA, Snoeys J, Upreti VV, Zheng M, and Hall SD (2015) Physiologically based pharmacokinetic modeling in drug discovery and development: a pharmaceutical industry perspective. *Clin Pharmacol Ther* **97:**247-262.

Kenny JR, Ramsden D, Buckley DB, Dallas S, Fung C, Mohutsky M, Einolf HJ, Chen L, Dekeyser JG, Fitzgerald M, Goosen TC, Siu YA, Walsky RL, Zhang G, Tweedie D, and Hariparsad N (2018) Considerations from the Innovation and Quality Induction Working Group in Response to Drug-Drug Interaction Guidances from Regulatory Agencies: Focus on CYP3A4 mRNA In Vitro Response Thresholds, Variability, and Clinical Relevance. *Drug Metab Dispos* **46:**1285-1303.

Kharasch ED, Walker A, Hoffer C, and Sheffels P (2004) Intravenous and oral alfentanil as in vivo probes for hepatic and first-pass cytochrome P450 3A activity: noninvasive assessment by use of pupillary miosis. *Clin Pharmacol Ther* **76:**452-466.

Kinirons MT, Lang CC, He HB, Ghebreselasie K, Shay S, Robin DW, and Wood AJ (1996) Triazolam pharmacokinetics and pharmacodynamics in Caucasians and Southern Asians: ethnicity and CYP3A activity. *Br J Clin Pharmacol* **41:**69-72.

Kirby BJ, Collier AC, Kharasch ED, Whittington D, Thummel KE, and Unadkat JD (2011) Complex drug interactions of HIV protease inhibitors 1: inactivation, induction, and inhibition of cytochrome P450 3A by ritonavir or nelfinavir. *Drug Metab Dispos* **39:**1070-1078.

Lazarou J, Pomeranz BH, and Corey PN (1998) Incidence of adverse drug reactions in hospitalized patients: a meta-analysis of prospective studies. *JAMA* **279:**1200-1205.

Lu C and Li AP (2001) Species comparison in P450 induction: effects of dexamethasone, omeprazole, and rifampin on P450 isoforms 1A and 3A in primary cultured hepatocytes from man, Sprague-Dawley rat, minipig, and beagle dog. *Chem Biol Interact* **134:**271-281.

Ly JQ, Messick K, Qin A, Takahashi RH, and Choo EF (2017) Utility of CYP3A4 and PXR-CAR-CYP3A4/3A7 Transgenic Mouse Models To Assess the Magnitude of CYP3A4 Mediated Drug-Drug Interactions. *Mol Pharm* **14:**1754-1759.

Magro L, Moretti U, and Leone R (2012) Epidemiology and characteristics of adverse drug reactions caused by drug-drug interactions. *Expert Opin Drug Saf* **11:**83-94.

Mouly S, Lown KS, Kornhauser D, Joseph JL, Fiske WD, Benedek IH, and Watkins PB (2002) Hepatic but not intestinal CYP3A4 displays dose-dependent induction by efavirenz in humans. *Clin Pharmacol Ther* **72:**1-9.

Nelson DR, Zeldin DC, Hoffman SM, Maltais LJ, Wain HM, and Nebert DW (2004) Comparison of cytochrome P450 (CYP) genes from the mouse and human genomes, including nomenclature recommendations for genes, pseudogenes and alternative-splice variants. *Pharmacogenetics* **14:**1-18.

Oktora MP, Denig P, Bos JHJ, Schuiling-Veninga CCM, and Hak E (2019) Trends in polypharmacy and dispensed drugs among adults in the Netherlands as compared to the United States. *PLoS One* **14:**e0214240.

Perloff MD, von Moltke LL, Court MH, Kotegawa T, Shader RI, and Greenblatt DJ (2000) Midazolam and triazolam biotransformation in mouse and human liver microsomes: relative contribution of CYP3A and CYP2C isoforms. *J Pharmacol Exp Ther* **292:**618-628.

Peters SA and Dolgos H (2019) Requirements to Establishing Confidence in Physiologically Based Pharmacokinetic (PBPK) Models and Overcoming Some of the Challenges to Meeting Them. *Clin Pharmacokinet* **58:**1355-1371.

Pirmohamed M, James S, Meakin S, Green C, Scott AK, Walley TJ, Farrar K, Park BK, and Breckenridge AM (2004) Adverse drug reactions as cause of admission to hospital: prospective analysis of 18 820 patients. *BMJ* **329:**15-19.

Ramsden D, Zhou J, and Tweedie DJ (2015) Determination of a Degradation Constant for CYP3A4 by Direct Suppression of mRNA in a Novel Human Hepatocyte Model, HepatoPac. *Drug Metab Dispos* **43:**1307-1315.

RIFADIN (2020) Bridgewater, in: *Sanofi-Aventis, LLC* (NJ ed.

Shebley M, Sandhu P, Emami Riedmaier A, Jamei M, Narayanan R, Patel A, Peters SA, Reddy VP, Zheng M, de Zwart L, Beneton M, Bouzom F, Chen J, Chen Y, Cleary Y, Collins C, Dickinson GL, Djebli N, Einolf HJ, Gardner I, Huth F, Kazmi F, Khalil F, Lin J, Odinecs A, Patel C, Rong H, Schuck E, Sharma P, Wu SP, Xu Y, Yamazaki S, Yoshida K, and Rowland M (2018) Physiologically Based Pharmacokinetic Model Qualification and Reporting Procedures for Regulatory Submissions: A Consortium Perspective. *Clin Pharmacol Ther* **104:**88-110.

Shimada T, Mimura M, Inoue K, Nakamura S, Oda H, Ohmori S, and Yamazaki H (1997) Cytochrome P450-dependent drug oxidation activities in liver microsomes of various animal species including rats, guinea pigs, dogs, monkeys, and humans. *Arch Toxicol* **71:**401-408.

Shimada T, Yamazaki H, Mimura M, Inui Y, and Guengerich FP (1994) Interindividual variations in human liver cytochrome P-450 enzymes involved in the oxidation of drugs, carcinogens and toxic chemicals: studies with liver microsomes of 30 Japanese and 30 Caucasians. *J Pharmacol Exp Ther* **270:**414-423.

Shou M, Hayashi M, Pan Y, Xu Y, Morrissey K, Xu L, and Skiles GL (2008) Modeling, prediction, and in vitro in vivo correlation of CYP3A4 induction. *Drug Metab Dispos* **36:**2355-2370.

SUSTIVA (2015) Princeton, in: *Bristol-Meyers Squibb* (NJ ed.

Takahashi RH, Shahidi-Latham SK, Wong S, and Chang JH (2017) Applying Stable Isotope Labeled Amino Acids in Micropatterned Hepatocyte Coculture to Directly Determine the Degradation Rate Constant for CYP3A4. *Drug Metab Dispos* **45:**581-585.

van Waterschoot RA, van Herwaarden AE, Lagas JS, Sparidans RW, Wagenaar E, van der Kruijssen CM, Goldstein JA, Zeldin DC, Beijnen JH, and Schinkel AH (2008) Midazolam metabolism in cytochrome P450 3A knockout mice can be attributed to up-regulated CYP2C enzymes. *Mol Pharmacol* **73:**1029-1036.

Wagner C, Pan Y, Hsu V, Sinha V, and Zhao P (2016) Predicting the Effect of CYP3A Inducers on the Pharmacokinetics of Substrate Drugs Using Physiologically Based Pharmacokinetic (PBPK) Modeling: An Analysis of PBPK Submissions to the US FDA. *Clin Pharmacokinet* **55:**475-483.

Wienkers LC and Heath TG (2005) Predicting in vivo drug interactions from in vitro drug discovery data. *Nat Rev Drug Discov* **4:**825-833.

Xie W, Barwick JL, Downes M, Blumberg B, Simon CM, Nelson MC, Neuschwander-Tetri BA, Brunt EM, Guzelian PS, and Evans RM (2000) Humanized xenobiotic response in mice expressing nuclear receptor SXR. *Nature* **406:**435-439.

Yang J, Liao M, Shou M, Jamei M, Yeo KR, Tucker GT, and Rostami-Hodjegan A (2008) Cytochrome p450 turnover: regulation of synthesis and degradation, methods for determining rates, and implications for the prediction of drug interactions. *Curr Drug Metab* **9:**384-394.

Zhang JG, Ho T, Callendrello AL, Clark RJ, Santone EA, Kinsman S, Xiao D, Fox LG, Einolf HJ, and Stresser DM (2014) Evaluation of calibration curve-based approaches to predict clinical inducers and noninducers of CYP3A4 with plated human hepatocytes. *Drug Metab Dispos* **42:**1379-1391.

Footnotes

Financial Disclosure: This work received no external funding.

Declaration of interest: The authors declare no conflict of interest.

DMD Fast Forward. Published on April 16, 2021 as DOI: 10.1124/dmd.121.000439
This article has not been copyedited and formatted. The final version may differ from this version.

Figure Legends

Figure 1. Blood concentration-time profile in Tg-Composite animals following oral administration of A) rifampin at 3, 10, 30 and 100 mg/kg, B) efavirenz at 5, 15, 50 and 250 mg/kg, and C) pioglitazone at 1, 5, 50, and 200 mg/kg. Starting with the lowest dose, the first dose is shown as inverted orange triangle, the second dose is shown as green circle, the third dose is shown as blue triangle and the highest dose is shown as purple square. Data are presented as mean $\pm$ SD (N=4).

Figure 2. Concentration-response curve when plotting CYP3A activity against in vivo response in Tg-Composite animals following oral administration of A) rifampin at 3, 10, 30 and 100 mg/kg, B) efavirenz at 5, 15, 50 and 250 mg/kg, and C) pioglitazone at 1, 5, 50, and 200 mg/kg. In vivo CYP3A activity was determined by monitoring changes in triazolam AUC_{tlast} when Tg-Composite animals were treated with vehicle or perpetrators (AUC_{veh}/AUC_{treat}). In vivo perpetrator concentrations that were used was Cmax or Cavg calculated from AUC_{tlast}. Cmax is shown as blue filled circles and Cavg is shown as filled green square. Mean data for in vivo CYP3A activity and perpetrator concentrations were plotted.

Figure 3. Concentration-response curve when plotting CYP3A activity against in vitro response in microsomes prepared from Tg-Composite animals following oral administration of A) rifampin at 3, 10, 30 and 100 mg/kg, B) efavirenz at 5, 15, 50 and 250 mg/kg, and C) pioglitazone at 1, 5, 50, and 200 mg/kg. In vitro CYP3A activity was determined in microsomes by monitoring fold-increase in triazolam enzymatic activity (k_{treat}/k_{veh}). In vivo perpetrator concentrations that were used was Cmax or Cavg calculated from AUC_{tlast}. Cmax is shown as blue open circles and Cavg is shown as open green square. Mean data for in vitro CYP3A activity and perpetrator concentrations were plotted.

Table 1. Summary of mean AUC_{tlast}, C_{max} and C_{avg} values (± SD), following oral administration of rifampin, efavirenz and pioglitazone, in Tg-Composite animals (N=4)

	Rifampin				Efavirenz				Pioglitazone			
Dose (mg/kg)	3	10	30	100	5	15	50	250	1	5	50	200
AUC_{tlast} (µM*hr)	0.643 (0.571)	4.32 (1.06)	14.1 (5.2)	141 (60)	0.0217 (0.0148)	0.112 (0.068)	1.06 (0.16)	2.29 (0.70)	3.82 (0.53)	11.0 (1.2)	54.5 (6.6)	104 (32)
Cavg (µM)	0.0804 (0.0071)	0.540 (0.132)	1.76 (0.69)	17.6 (7.6)	0.0217 (0.0022)	0.0373 (0.0085)	0.177 (0.020)	0.286 (0.088)	0.478 (0.066)	1.38 (0.16)	6.81 (0.82)	13.0 (4.0)
Cmax (µM)	0.0963 (0.0101)	0.655 (0.110)	2.33 (0.75)	25.1 (11.1)	0.0561 (0.0170)	0.150 (0.129)	0.933 (1.158)	2.46 (1.13)	1.19 (0.16)	4.68 (0.57)	16.7 (5.3)	32.0 (10.8)

DMD Fast Forward. Published on April 16, 2021 as DOI: 10.1124/dmd.121.000439
This article has not been copyedited and formatted. The final version may differ from this version.

Table 2. Summary of mean changes CYP3A activity measured as triazolam AUC ratio (± SD) reported as AUC_{veh}/AUC_{treat} for in vivo, and triazolam in vitro activity (± SD) reported as fold-increase relative to vehicle control, following oral administration of rifampin, efavirenz and pioglitazone to Tg-Composite animals (N=4)

	Dose (mg/kg)	In Vivo AUC Ratio (AUC_{veh}/AUC_{treat})	In Vitro Activity (Fold-Increase Relative to Vehicle Control)
Rifampin	3	2.78 (1.51)	2.75 (0.91)
	10	13.0 (6.53)	4.75 (1.79)
	30	24.6 (14.5)	9.87 (2.49)
	100	44.9 (26.9)	11.0 (2.77)
Efavirenz	5	1.05 (0.47)	0.978 (0.414)
	15	1.42 (0.62)	1.19 (0.52)
	50	1.90 (0.82)	2.08 (0.833)
	250	5.59 (1.98)	4.22 (1.82)
Pioglitazone	1	1.17	1.07

DMD Fast Forward. Published on April 16, 2021 as DOI: 10.1124/dmd.121.000439
This article has not been copyedited and formatted. The final version may differ from this version.

		(0.49)	(0.13)
	5	1.19 (0.38)	1.17 (0.17)
	50	1.43 (0.53)	1.52 (0.23)
	200	1.61 (0.51)	1.66 (0.16)

Table 3. Summary of EC50 and Emax determined from concentration-response curve using mean in vivo change in AUC ratio (AUC_{veh}/AUC_{treat}) or fold-increase of in vitro CYP3A activity relative to vehicle control (k_{treat}/k_{veh}), and in vivo Cmax or Cavg of rifampin, efavirenz and pioglitazone determined in Tg-Composite animals

		Rifampin		Efavirenz		Pioglitazone	
		EC50 (μM)	Emax (Fold Induction)	EC50 (μM)	Emax (Fold Induction)	EC50 (μM)	Emax (Fold Induction)
Cavg	In Vivo	1.76	49.2	Not calculated		7.69	1.89
	In Vitro	0.708	11.8	Not calculated		5.99	1.97
Cmax	In Vivo	2.24	48.6	Not calculated		27.5	2.08
	In Vitro	0.882	11.8	Not calculated		20.5	2.10

DMD Fast Forward. Published on April 16, 2021 as DOI: 10.1124/dmd.121.000439
This article has not been copyedited and formatted. The final version may differ from this version.

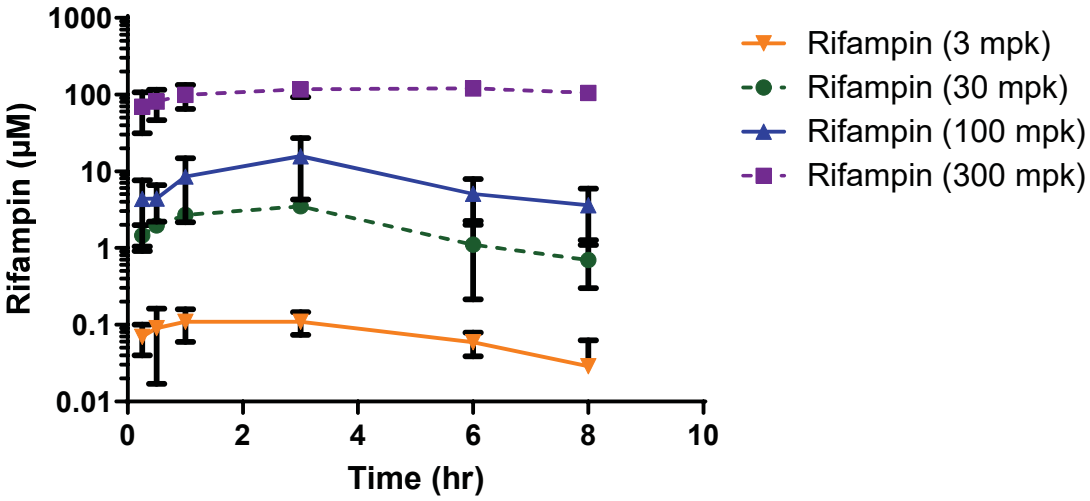

Figure 1A

DMD Fast Forward. Published on April 16, 2021 as DOI: 10.1124/dmd.121.000439
This article has not been copyedited and formatted. The final version may differ from this version.

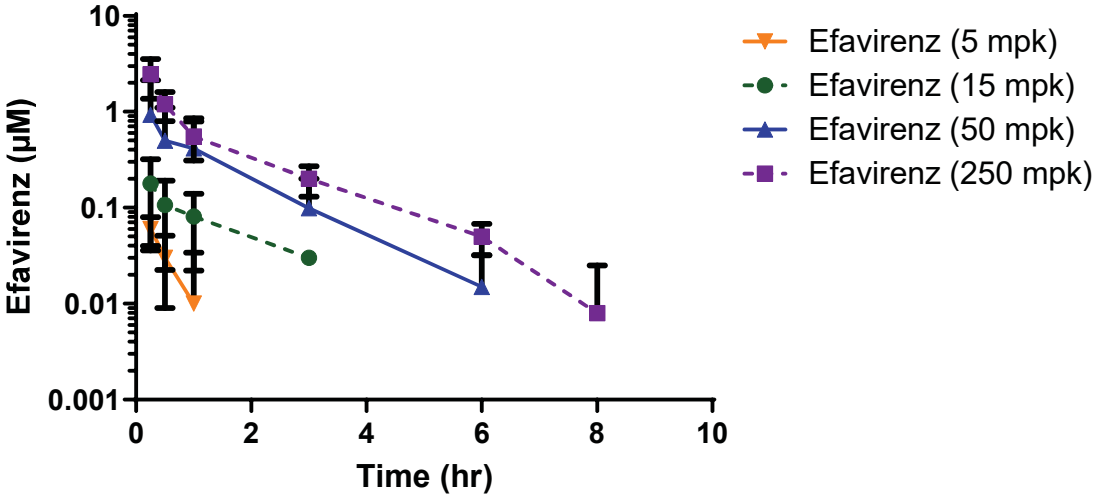

Figure 1B

DMD Fast Forward. Published on April 16, 2021 as DOI: 10.1124/dmd.121.000439
This article has not been copyedited and formatted. The final version may differ from this version.

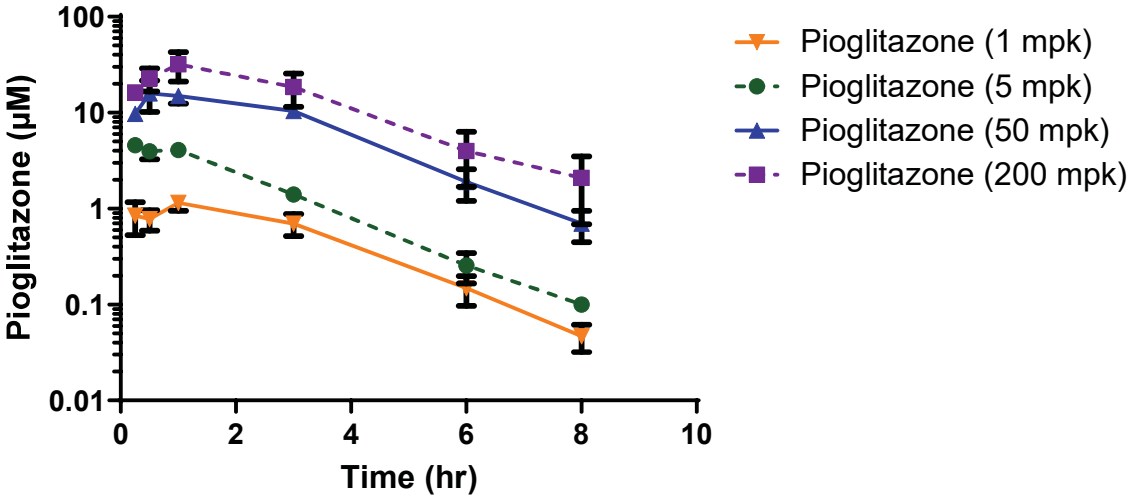

Figure 1C

DMD Fast Forward. Published on April 16, 2021 as DOI: 10.1124/dmd.121.000439
This article has not been copyedited and formatted. The final version may differ from this version.

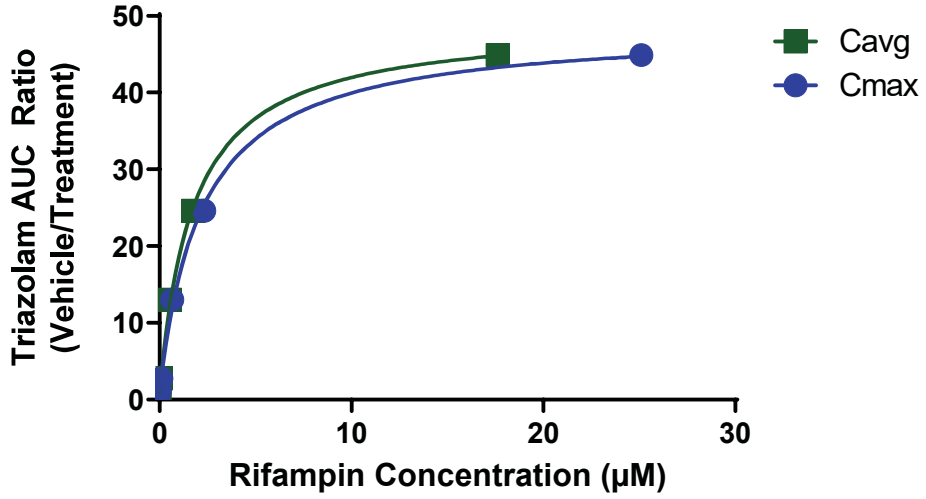

Figure 2A

DMD Fast Forward. Published on April 16, 2021 as DOI: 10.1124/dmd.121.000439
This article has not been copyedited and formatted. The final version may differ from this version.

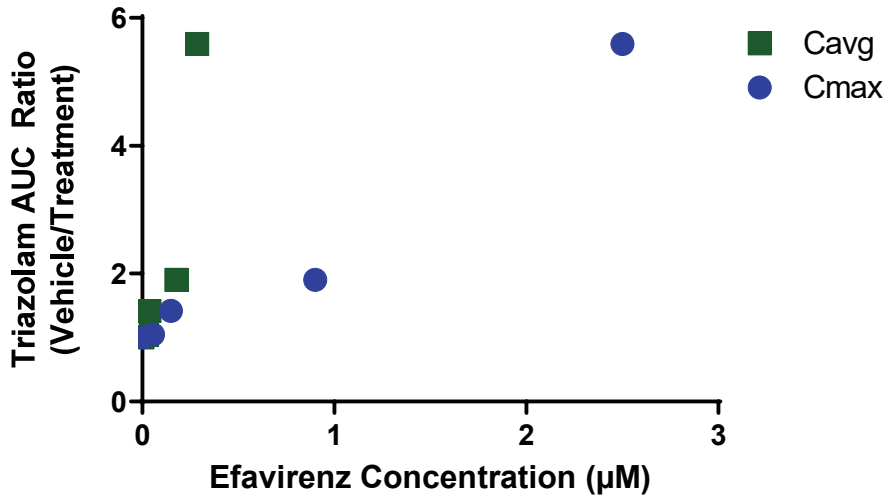

Figure 2B

DMD Fast Forward. Published on April 16, 2021 as DOI: 10.1124/dmd.121.000439
This article has not been copyedited and formatted. The final version may differ from this version.

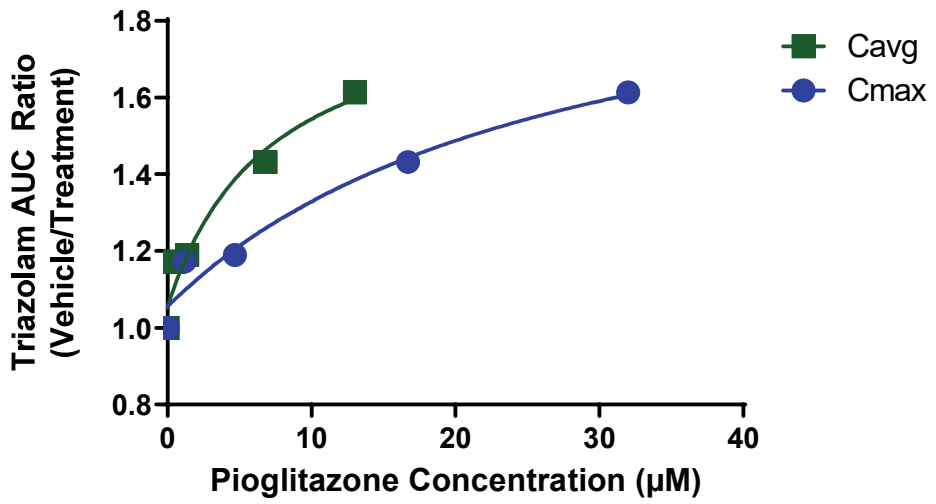

Figure 2C

DMD Fast Forward. Published on April 16, 2021 as DOI: 10.1124/dmd.121.000439
This article has not been copyedited and formatted. The final version may differ from this version.

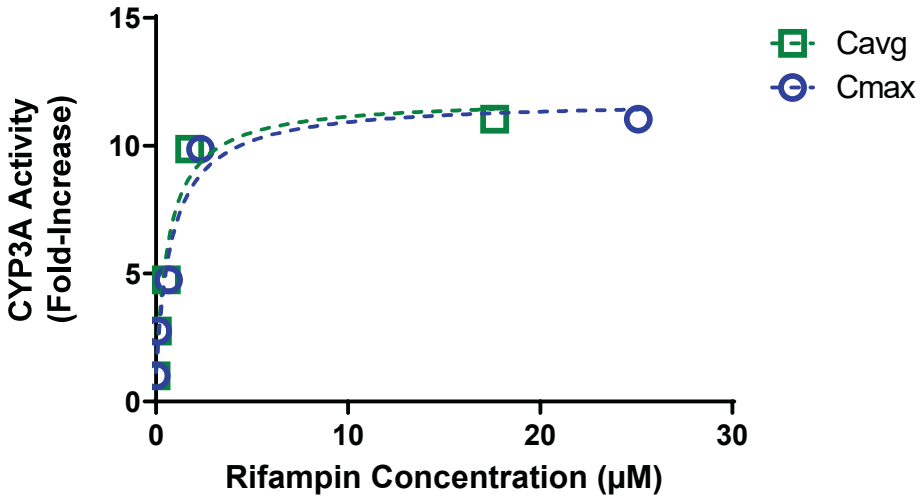

Figure 3A

DMD Fast Forward. Published on April 16, 2021 as DOI: 10.1124/dmd.121.000439
This article has not been copyedited and formatted. The final version may differ from this version.

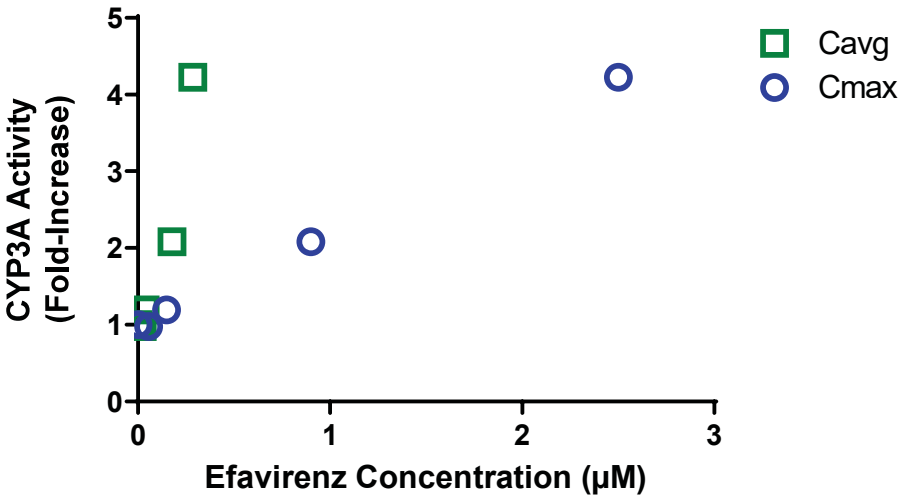

Figure 3B

DMD Fast Forward. Published on April 16, 2021 as DOI: 10.1124/dmd.121.000439
This article has not been copyedited and formatted. The final version may differ from this version.

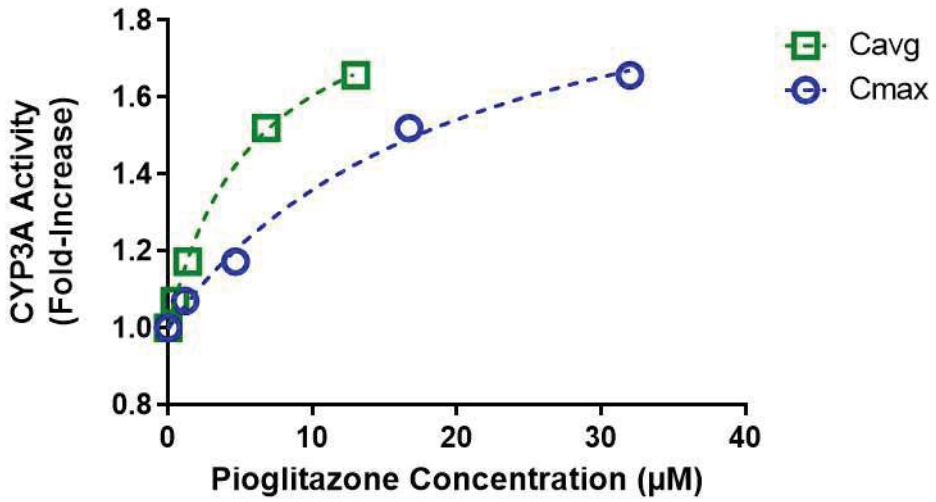

Figure 3C